Journal of the Korean Vacuum Society
Vol. 2, No. 3, September 1993, pp. 360-367

〈연구논문〉

Deposition Mechanism of Tungsten thin Film in LPCVD System

Sung Hoon Kim and Se Ahn Song*

Department of Chemistry, Seoul National University, Seoul 151-741, Korea
†Precision Analysis Center, Samsung Advanced Institute of Technology, P.O. Box 111, Suwon 440-600, Korea

(Received June 4, 1993)

저압 화학 기상 증착에서의 텅스텐 박막 증착 메카니즘

김성훈 · 송세안*

서울대학교 자연과학대학 화학과
†삼성종합기술원 그룹시험분석센타

(1993년 6월 4일 접수)

Abstract – As a first step to determine the deposition mechanism of tungsten thin film, we investigated the thermodynamics of SiH_4 and WF_6 thermal decomposition and the surface catalysis reaction. In experiment we deposited tungsten thin film on Si(100) substrate by using the LPCVD (low pressure chemical vapor deposition) technique. WF_6 was used as a source gas for tungsten and SiH_4 was used as a reducing gas for WF_6. Reduction of WF_6 by both Si substrate and SiH_4 was investigated. During the reaction, we monitored the variation of thin film surface. We also analyzed thin film morphology. From the theoretical considerations and obtained experimental results, we concluded that tungsten was deposited by Si substrate reduction of WF_6 and the subsequent SiH_4 reduction of WF_6.

요 약 – 텅스텐 박막 증착의 메카니즘을 밝히기 위하여 먼저 SiH_4와 WF_6의 열분해 반응에 관한 열역학적 결과들과 표면 촉매 반응에 대한 이론적인 결과들을 고찰하였다. 실험적으론 저압 화학 기상 증착법을 이용하여 WF_6를 SiH_4로 환원시켜 텅스텐 박막을 Si(100) 기판위에 증착하였으며 증착 반응 중의 기판 표면의 변화를 *in-situ*로 측정하였다. 증착 메카니즘을 밝히기 위하여 반응기체를 WF_6, SiH_4, WF_6+SiH_4, $WF_6 \rightarrow SiH_4 \rightarrow WF_6+SiH_4$로 달리하여 반응시켰으며 그 때의 박막 특성과 표면 및 단면 형상을 측정하였다. 이론적인 고찰과 실험적인 결과들로부터 텅스텐 박막은 먼저 Si 기판에 의한 WF_6의 환원반응으로 인한 증착과 이어서 SiH_4에 의한 WF_6의 환원으로 증착됨을 밝혔다.

1. Introduction

As the VLSI system becomes more complicated, the development of semiconductor material and the study of thin film deposition become increasingly crucial. For the development of semiconductor materials, refractory metals, expecially tungsten, are regarded as promising candidates to replace aluminum and polysilicon[1-3]. Generally the study on the tungsten thin film deposition is classified into selective tungsten deposition utilizing the selectivity of tungsten deposition only on silicon (and not on silicon oxide) and blanket tungsten deposition experiment[4]. In selective tungsten deposition expe-

*Author to whom correspondence should be addressed (Present address: New Materials LAB, Samsung Advanced Institute of Technology, P.O. Box 111, Suwon 440-600, Korea)

riment the goal is mainly to achieve better selectivity, which is typically deteriorated by the presence of halogen atoms such as fluorine[5, 6]. In blanket tungsten deposition the goal is mainly to improve thin film characteristics such as uniformity, crystallinity, physical and electrical properties[5, 6]. In both cases knowledge of the deposition mechanism is necessary to improve selectivity or characteristics of the resulting tungsten thin film.

In theoretical consideration we investigated the thermodynamics of the SiH_4 and WF_6 thermal decomposition. In experiment we deposited tungsten thin film on *p*-(100) Si substrate by SiH_4 reduction of WF_6 in LPCVD system. During the reaction, we monitored the variation of thin film surface by our home made *in-situ* surface monitor. We suggested the deposition mechanism of tungsten thin film from the theoretical considerations and the experimental results.

2. Experimental

The LPCVD system of cold-wall type is shown in Fig. 1. The reactor wall was water-cooled. The temperature of resistance heater was uniformly controlled during the reaction using the K type thermocouple (Chromel-Alumel) and a temperature controller (Omega 4001KC). WF_6 (99.999%, Takachiho) was used without further purification. Flow rates of WF_6 was controlled by MFC (mass flow controller). A 100-mm diameter *p*-(100) Si wafer was used, following pretreament with 10% HF buffer solution for 1 min., then drying with nitrogen gas. As shown in Fig. 2 a home-made in-situ surface monitor was constructed by using a He-Ne laser and a photodiode detector with monochromator.

Film surface and cross section were examined by SEM (scanning electron microscopy, Jeol JSM 840) and TEM (transmission electron microscopy, Hitachi H9000, 300 kV). Composition was deduced by EDX (energy dispersive x-ray spectrometry) spectrum and crystal structure was determined from XRD (X-ray diffraction, JEOL DX-GD-2) spectrum. Film thickness was measured by Dektak. For the detailed study of the deposition mechanism, we executed tungsten thin film deposition experiment according to the different source gas conditions as shown in Table 1.

3. Results and Discussion

3.1. Thermodynamics of SiH_4 and WF_6 Thermal Decomposition

In LPCVD condition SiH_4 is decomposed and forms Si(*s*) as in the following reaction.

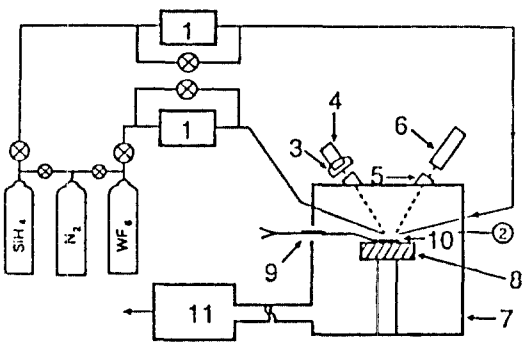

1. Mass flow controller 2. Pressure gauge
3. Monochromator 4. Photo diode
5. Sapphire window 6. He-Ne laser
7. Reactor 8. Heater
9. Thermocouple 10. Substrate (Si wafer)
11. Pump

Fig. 1. Schematic diagram of LPCVD system.

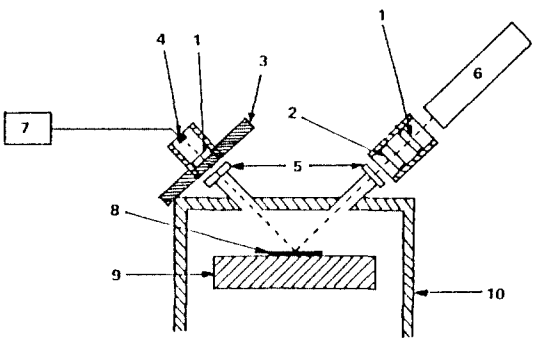

1. Rotatable linear polarizer
2. Quarter wave compensator
3. Monochromator 4. Photo diode
5. Sapphire windown 6. He-Ne laser
7. Digital volt meter 8. Substrate
9. Heater 10. Reactor

Fig. 2. Schematic diagram of surface monitoring system.

$SiH_4(g) \rightarrow Si(s)+2H_2(g)$ $\Delta H°=-8.2$ kcal/mol

As the reaction temperature is increased, the decomposition of SiH_4 is increased because the entropy change of this reaction is positive ($\Delta S°=17.7$ e.u.). Table 2 gives thermodynamic data for the reaction which can occur in SiH_4 decomposition reaction. The SiH_4 decomposition reaction can have the following initial reaction steps.

$SiH_4 \rightarrow SiH_3+H$ $\Delta H°=91.7$ kcal/mol
$SiH_4 \rightarrow SiH_2+2H$ $\Delta H°=165$ kcal/mol
$SiH_4 \rightarrow SiH_2+H_2$ $\Delta H°=60.8$ kcal/mol

Since the last reaction requires the least energy, we assume that SiH_4 is decomposed and form SiH_2+H_2 initially. The newly formed SiH_2 is then also decomposed and eventually forms $Si(s)+H_2$ ($\Delta H°=69$ kcal/mol).

From only thermodynamic point of view the decomposition of WF_6 is possible only above 2500 K ($WF_6(g) \rightarrow WF_5(g)+F(g)$ $\Delta H°=135$ kcal/mol, $\Delta S°=45$ e.u.). On the other hand, the reaction of WF_6 with $Si(s)$ is thermodynamically possible at any reaction temperatures ($WF_6(g)+3/2Si(s) \rightarrow W(s)+3/2\ SiF_4(g)$ $\Delta H°=-183$ kcal/mol, $\Delta S°=22$ e.u.). Table 3 gives thermodynamics data relevant to tungsten

Table 2. Thermodynamic constants of compounds which are related to SiH_4 thermal decomposition

Compounds	$\Delta H°_f$ (kcal/mol)	$C°_p$ (cal/mol deg^{-1})	$S°$ (cal/mol deg^{-1})	Ref.
SiH_4	7.3± 0.3	48.8	10.27	[7]
	8.2			[10]
SiH_3	47.8	51.7	9.6	[9]
SiH_2	58.0	49.4	8.3	[9]
	69± 3			[8]
SiH	91.7	44.2	7.0	[9]
$Si(g)$	107.7	40.1	5.3	[10]
$Si(s)$	0	4.5	4.8	[10]
Si_2H_6	19.1	65.4	19.1	[9]
Si_2H_5	55.7	69.6	18.1	[9]
H_3SiSiH	80.2	67.5	16.5	[9]
H_2SiSiH_2	57.4	65.3	16.9	[9]
Si_2H_3	105.7	66.1	15.3	[9]
Si_2H_2	83.5	58.7	10.5	[9]
$Si_2(g)$	141	54.9	8.1	[10]
Si_3H_8	28.9	83.2	28.2	[9]
$Si_3(g)$	152	64.0	13.2	[9]
H_2	0.0	31.2	6.9	[10]
H	52.1	27.4	5.0	[10]

Table 1. Experimental conditions for each scheme

Conditions/Scheme	1	2	3	4
Source gas	WF_6	SiH_4	WF_6+SiH_4	$WF_6 \rightarrow SiH_4 \rightarrow WF_6+SiH_4$
Flow rate (sccm)	36	18	WF_6 : 36, SiH_4 : 18	WF_6 : 36, SiH_4 : 18
Reaction Temp. (℃)	450	450	450	450
Total Pressure (mTorr)	150	100	250	150→100→250
Reaction Time (min.)	30	30	30	30→30→30
No. of runs	20	25	17	5

Table 3. Thermodynamic constants of compounds which are related to tungsten deposition[10]

Compounds		WF_6	$W(s)$	$HF(g)$	$SiF_4(g)$	$WF_5(g)$[11]
$\Delta H°_f$ (kcal/mol)		−411.5	0	−65.14	−396.0	−328.6
$S°$ (cal/mol deg)		81.504	7.8	41.5	67.43	79
$C°_p$ cal/mol deg	300°K	28.52	5.811	6.96	17.61	26.4 e.u. (300~500℃)
	400	31.65	5.96	6.97	19.85	
	500	33.50	6.06	6.97	21.40	
	600	34.66	6.16	6.99	22.48	
	700	35.41	6.27	7.02	23.22	
	800	35.93	6.37	7.10	23.76	
	900	36.29	6.48	7.13	24.15	

deposition.

3.2. Decomposition Reaction of SiH_4 and WF_6

It was reported that gas phase thermal decomposition rate of SiH_4 was dependent on pressure with an Arrhenius behavior of k $(sec^{-1}) = 10^{14.5} e^{-55.9\ kcal/RT}$ [12]. The activation energy value of 55.9 kcal/mol suggests that the initial step of SiH_4 decomposition is $SiH_4 \rightarrow SiH_2 + H_2$, whose $\Delta H°$ is 60.8 kcal/mol. In this work we attempted to determine the initial step of SiH_4 thermal decomposition from the calculation of pressure dependence of the reaction rate from RRKM (Rice-Ramsperger-Kassel-Marcus) theory[13]. Table 4 gives the models of SiH_4 and $SiH_2 \cdots H_2$ complex with relevent RRKM input parameters. Table 5 and Fig. 3 show the results of RRKM calculation for thermal decomposition rate of SiH_4. The rate of the gas phase SiH_4 thermal decomposition is shown to decrease as the pressure drops. Under typical LPCVD condition of a few hundred millitorr of total pressure, the thermal decomposition rate is expected to be only 10^{-4} k . On the other hand, since the decomposition of WF_6 in gas phase is thermodynamically impossible below 2500 K, Si(s) substrate or reducing gas such as H_2

Table 4. Input parameters for RRKM calculations in $SiH_4 \rightarrow SiH_2 + H_2$ reactions

	Reactant	Activated complex
Model	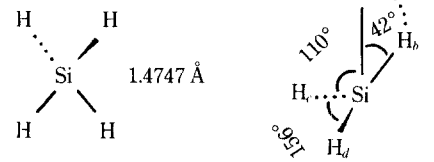	
Symmetry	Td	Cs
Frequency (cm^{-1})	2309, 2311(3), 1019(2), 1019(2)	307, 2288, 2199, 1716, 1205, 1062, 996, 774, 731
Moment of inertia	$I = 9.773 \times 10^{-24}$ g·Å^2	$I_a = 7.276 \times 10^{-24}$ g·Å^2 $I_b = 9.373 \times 10^{-24}$ g·Å^2 $I_c = 1.448 \times 10^{-24}$ g·Å^2
r(Å)	$r_{Si-H} = 1.4747$ Å	$r_{Si-H} = 1.6364$ Å 1.5149 Å 1.4765 Å $r_{H-H} = 1.135$ Å

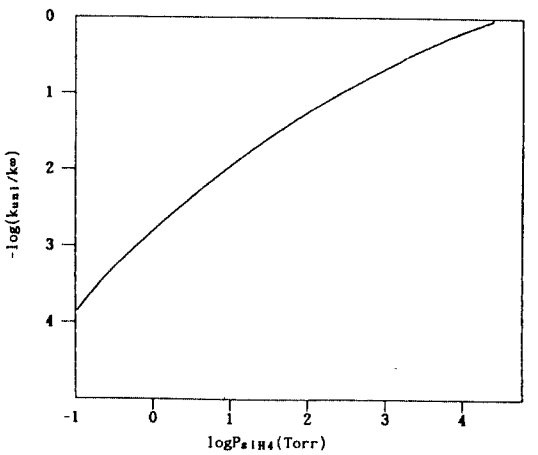

Fig. 3. RRKM thermal decomposition rate of SiH_4 as a function of SiH_4 pressure at 900 K.

Table 5. Results of RRKM calculation for the pressure dependence of SiH_4 thermal decomposition rate

Temp. (K)	β	$S°$	log$A$	k_∞	sec^{-1} k (700 torr)	sec^{-1} k (0.5 torr)
800	0.25	63.59	14.56	2.114×10^{-2}	6.866×10^{-3}	8.280×10^{-6}
820	0.25	64.03	14.57	4.834×10^{-2}	1.553×10^{-2}	1.863×10^{-5}
840	0.25	64.47	14.58	1.060×10^{-1}	3.369×10^{-2}	4.019×10^{-5}
860	0.25	64.90	14.59	2.234×10^{-1}	7.030×10^{-2}	8.341×10^{-4}
880	0.25	65.33	14.60	4.540×10^{-1}	1.414×10^{-1}	1.670×10^{-4}
900	0.25	65.75	14.61	8.916×10^{-1}	2.751×10^{-1}	3.232×10^{-4}
930	0.25	66.37	14.62	2.313	7.035×10^{-1}	8.208×10^{-4}
960	0.25	66.99	14.64	5.625	1.687	1.955×10^{-3}
990	0.25	67.59	14.65	12.89	3.814	4.392×10^{-3}
Activation energy (kcal/mol)					52.36	51.97

Table 6. Free energy changes (ΔG) of various reactions at 600 K [17]

Reactions	ΔG (kcal/mol)
$WF_6 + 1.5Si \rightarrow W + 1.5SiF_4$	−179.4
$WF_6 + 3H_2 \rightarrow W + 6HF$	−27.9
$WF_6 + 1.5SiH_4 \rightarrow W + 1.5SiF_4 + 3H_2$	−208.7
$WF_6 + 2.1SiH_4 \rightarrow 0.2W_5Si_3 + 1.5SiF_4 + 4.2H_2$	−227.6
$WF_6 + 3.5SiH_4 \rightarrow WSi_2 + 1.5SiF_4 + 7H_2$	−268.9

(*g*) or SiH_4(*g*) is used to decompose WF_6. In Si substrate reduction of WF_6, it is known that the initial tungsten deposition rate is rapid but decreases as the reaction proceeds because of the occupation of Si active sites on substrate surface by deposited tungsten[14]. The activation energy of this reaction is initially close to zero but increases as the reaction proceeds. Alternative to this self-limiting deposition, there are many reports of tungsten thin film deposition through the reduction of WF_6 by reducing gas (H_2)[15, 16]. The mechanism of this reaction is usually taken as a two-step mechanism: reduction of WF_6 by Si substrate and subsequent H_2 reduction of WF_6[16]. It was also reported that the value of ΔG for WF_6-Si reduction (−179 kcal/mol at 600 K) is lower than that for WF_6-H_2 reduction (−28 kcal/mol at 600 K) (Table 6). This supports the well-known two step mechanism in the case of WF_6-H_2 reduction. In the case of WF_6-SiH_4, however, it is reported that encroachment is weak and the value of ΔG (−209 kcal/mol at 600 K) is similar to that of WF_6-Si reaction, so that both one step and two step mechanisms are quite possible. Up to present, the mechanism of this reaction is not known in detail. The only clue comes from the suggestion of Schmitz that this mechanism involves a heterogeneous reaction, that is WF_6 and SiH_4 are initially adsorbed on Si substrate separately and then reduction reaction proceeds on substrate surface[18].

3.3. Deposition of Tungsten Thin Film from SiH_4 Reduction of WF_6

Several workers showed that under normal conditions there is no consumption of Si substrate in SiH_4 reduction of WF_6[19, 20]. This means that SiH_4 reduction of WF_6 is proceeded by one step reaction,

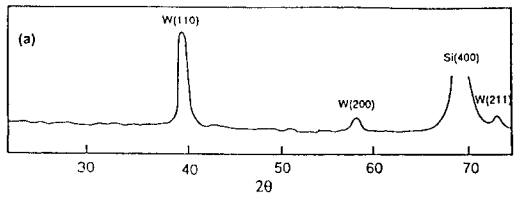

Fig. 4. XRD spectrum of tungsten thin film.

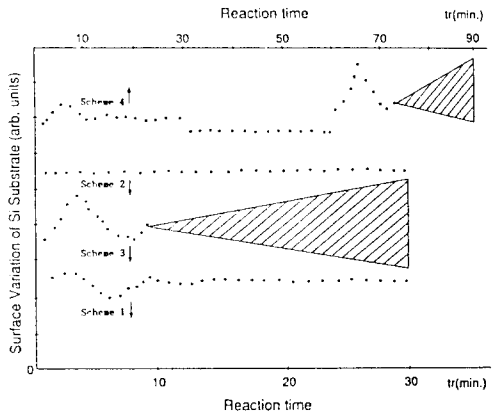

Fig. 5. Surface variation with reaction time for each reaction scheme. Shield areas show the range of output signal with different runs.

bypassing the reduction step by the Si substrate. We then proceeded to verify whether a one step or two step process is involved by deposition of tungsten according to the following four different schemes of using source gases, i.e., WF_6 only (Scheme 1), SiH_4 only (Scheme 2), $WF_6 + SiH_4$ (Scheme 3) and $WF_6 \rightarrow SiH_4 \rightarrow WF_6 + SiH_4$ (Scheme 4). The conditions are given in Table 1. Fig. 4 is the XRD spectrum of deposited thin film. Three peaks, located at tungsten (110), (200), and (211) positions, are evident and indicate that alpha phase of tungsten (α-W) was formed[21]. By using the *in-situ* surface monitor the incubation period and the change in surface characteristics were monitored and the results are shown in Fig. 5. In Scheme 2 no surface variation was observed. In Schemes 1, 3 and 4 the incubation period is alike. Thus it is conjectured that in Scheme 2 no Si or SiH_x is deposited but in Schemes 1, 3 and 4 same initial reaction (such as Si substrate reduction of WF_6) occurs. The incubation period decreases with the increase of WF_6 flow rate, but, it does not vary

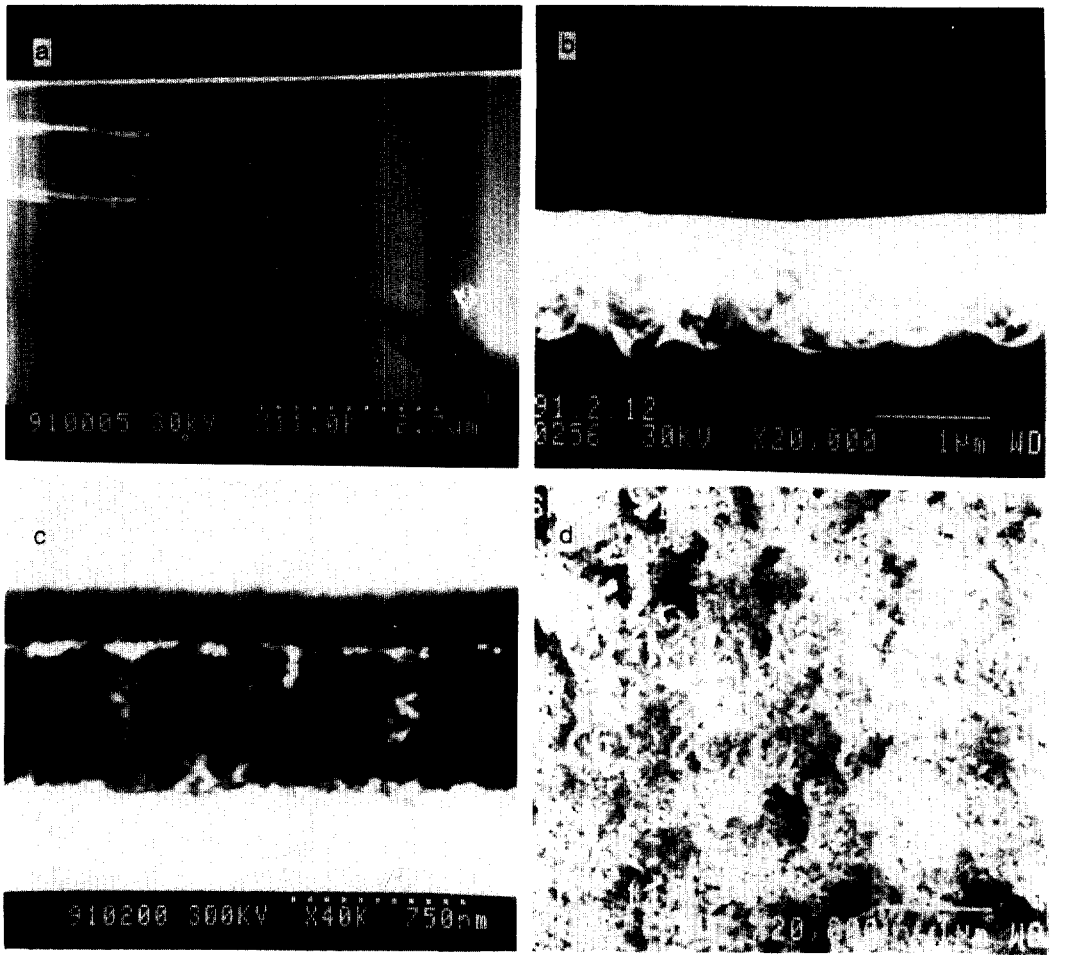

Fig. 6. (a) SEM micrograph of cross section for Scheme 1. (b) SEM micrograph of cross section for Scheme 3. (c) TEM micrograph of cross section for Scheme 4. (d) SEM micrograph of Si substrate surface from which deposited tungsten film was peeled off.

with SiH_4 flow rate in WF_6+SiH_4 mixture. The incubation period also decreases with the increase of reaction temperature and total pressure. These results show explicit dependence of incubation period on WF_6 flow rate and the collision number between WF_6 and substrate, but not on the SiH_4 flow rate. Therefore it is surmised that the initial deposition reaction involves a reaction between Si substrate and the gas phase WF_6.

Figs. 6(a), (b), and (c) show the cross sectional SEM and TEM images in Schemes 1, 3 and 4. The Si substrate reduction of WF_6, usually called displacement reaction, only produces self-limited thin film (~300 Å) as shown in Fig. 6(a). This result has been shown by Busta according to native oxide thickness[21]. Fig. 6(d) shows the SEM micrograph of Si substrate surface where W film is peeled off. This image gives an evidence for chemical reactions between Si substrate and source gas of tungsten (WF_6 in the present study). This is also supported by the roughness of interface between tungsten and Si substrate as seen in Figs. 6(b) and (c).

3.4. Deposition Mechanism in Catalysis Reaction

We can classify the deposition mechanism of tungsten thin film according to the well-known surface catalysis models. In bimolecular processes sur-

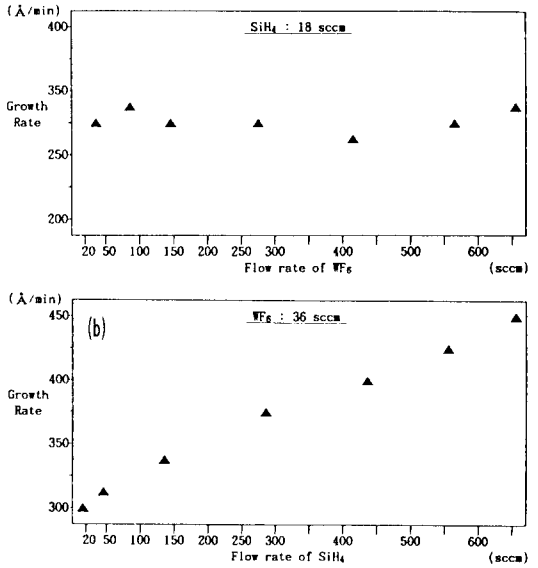

Fig. 7. Thin film growth rate as a function of partial pressures of (a) WF_6 and (b) SiH_4.

face catalysis reactions are generally considered to follow either the Langmuir-Hinshelwood or the Rideal-Eley mechanism[22]. In the Lagmuir-Hinshelwood mechanism reactant gases, A and B, are adsorbed on neighboring sites of substrate. They then react with each other on surface and form product. In this mechanism the rate is proportional to the probability of A and B molecules are adsorbing on neighboring sites, which is proportional to the product of the fractions covered by A and by B. Therefore the reaction rate is given by $v=(k_2K_AK_BP_AP_B)/(1+K_AP_A+K_BP_B)^2$ where k_2: rate constant for bimolecular reaction, P: partial pressure of each molecule, K: equilibrium constant of each molecule for adsorption. If the pressure P_A is kept constant, and P_B is varied, the rate would change as follows: the rate first increases, passes through a maximum, and then decreases. On the other hand, in the Rideal-Eley mechanism reactant A is adsorbed on substance and then react with gas phase reactant B. In this mechanism the rate of reaction is proportional to the fraction of adsorbed A molecules and partial pressure of B molecules. Therefore the reaction rate is given by $v=(k_2K_AP_AP_B)/(1+K_AP_A+K_BP_B)$. If B is not at all adsorbed the rate equation becomes $v=(k_2K_AP_AP_B)/(1+K_AP_A)$. The rate becomes saturated in the limit of high partial pressure P_A and the rate is directly proportional to P_B. Fig. 7(a) and (b) show the thin film growth rates in this work when either WF_6 or SiH_4 flow rate is varied while the other is kept constant. The thin film growth rate was obtained as $v=k_2[SiH_4]^1[WF_6]^0$. We suggest from these results that tungsten is deposited primarily by the Rideal-Eley mechanism. In this condition the partial pressure P_{WF_6} is already very high, so the rate appears to be saturated when the flow rate of WF_6 is varied. Based on the above results, we propose that the W deposition in SiH_4 reduction reaction is proceeded by initial Si substrate reduction of WF_6 with subsequent SiH_4 reduction of WF_6.

Table 7 Heat of formation values for Si, W and their fluorides

Compounds	H_f (kJ/mole)	Ref.
Si	456	[23]
Si_2	594	[23]
Si_3	615	[23]
SiF	7	[23]
SiF_2	−619	[23]
SiF_3	−1051	[24, 25]
SiF_4	−1615	[23]
WF	410	[24]
WF_2	−86	[25]
WF_3	−507	[25]
WF_4	−960	[25, 26]
WF_5	−1293	[25]
WF_6	−1722	[23]

4. Conclusion

In the present work tungsten was deposited by a two-step process: first by Si substrate reduction of WF_6 (step I) and the subsequent SiH_4 reduction of WF_6 (step II). The detailed mechanism of step I is that WF_6 is first adsorbed on Si substrate surface, which already has a native oxide layer, then the adsorbed WF_6 is decomposed in reaction with Si diffusing from the bulk through the oxide layer of a few hundred Å thickness on Si substrate. In step II, WF_6 is first adsorbed on tungsten sites already deposited, then SiH_4 is decomposed to SiH_2+H_2 by catalytic reaction of adsorbed tungsten

and/or WF_6. In this case it is expected that the desorption of H_2 gas occurs immediately from substrate surface. As a reaction product, SiF_4 is formed from the reaction of SiH_2 with WF_6. Table 7 gives the heat of formation values of W, Si, and their compounds with F. We summarize the proposed mechanism in step I and step II as following.

Step I:

$$WF_6 \rightarrow WF_6(ad/si/o) \quad (\Delta H^\circ \cong 0 \text{ kcal/mol})$$

$$2WF_6(ad/si/o) + 3Si(s) \rightarrow 2W(ad) + 3SiF_4(g) \quad (\Delta H^\circ = \text{ca. } -335 \text{ kcal/mol})$$

Step II:

$$WF_6 \rightarrow WF_6(ad/w) \quad (\Delta H^\circ \cong 0 \text{ kcal/mol})$$

$$WF_6(ad/w) + SiH_4(g) \rightarrow WF_6(ad/w) + SiH_2(ad) + H_2(g) \quad (\Delta H^\circ = \text{ca. } 60 \text{ kcal/mol})$$

$$WF_6(ad/w) + SiH_2(ad) \rightarrow W(ad) + SiF_4(g, ad) + HF(g, ad) \quad (\Delta H^\circ = \text{ca. } -112 \text{ kcal/mol})$$

Acknowledgements

This work was supported by Korea Electronics of Telecommunications Research Institute. We thank Prof. S. K. Kim for helpful discussions.

References

1. E. Rosencher, S. Delage, Y. Campidelli and F. Arnaud d'Avtaya, *Electron. Lett.* **20**, 762 (1984).
2. N. E. Miller and I. Beinglass, *Solid State Technol.* **25**(12), 85 (1982).
3. J. M. Shaw and J. A. Amick, *RCA Rev.* **31**, 306 (1970).
4. A. Sherman, *Chemical Vapor deposition for Microelectronics* (Noyes Publications, New Jersey, 1987).
5. M. L. Green and R. A. Levy, *J. Electrochem. Soc.* **132**(5), 1243 (1985).
6. J. A. Carlisle, D. R. Chopra, T. R. Dillingham, B. Gnade and G. Smith, *J. Appl. Phys.* **65**(6), 2313 (1989).
7. R. Waish, *Acc. Chem. Res.* **14**, 246 (1981).
8. S. K. Shin and J. L. Beauchamp, *J. Phys. Chem.* **90**, 1507 (1986).
9. M. E. Coltrin, R. J. Kee and J. A. Miller, *J. Electrochem Soc.* **133**, 1206 (1986).
10. D. R. Stull *et al.*, *JANAF Thermochemical Tables*, 2nd ED. (NSRDS-NBS, 1971) p. 37.; R. C. Weast and M. J. Astle, *CRC Handbook of Chemistry and Physics* (CRC press Inc., 1979).
11. V. McCarty, W. E. Reith and M. T. Simon, *J. Elec. Soc.* **121**, 1372 (1974).
12. C. G. Newman, H. E. O'Neal, M. A. Ring, F. Leska and N. Shipley, *Int. J. Chem. Kinetics,* **11**, 1167 (1979).
13. P. J. Robinson and K. A. Holbrook, *Unimolecular Reactions* (Wiley Intersciences, New York, 1972).
14. E. K. Broadbent and C. L. Ramiller, *J. Electrochem. Soc.* **131**, 1427 (1984).
15. E. Kato and K. Itsumi, *J. Electron. Chem.* **135**(12), 3163 (1988).
16. R. A. Levy and M. L. Green, *J. Electrochem. Soc.* **134**(2), 37C (1987).
17. Y. Kusumoto, K. Takakuwa, H. Hashinokuchi, T. Ikuta and I. Nakayama, *Tungsten and Other Refractory Metals for VLSI Applications III,* edited by V. A. Wells (Materials Research Society, Pittsburgh, 1988) p. 103.
18. J. E. J. Schmitz, A. J. M. van Dijk and M. W. M. Graef, *Proceedings of 10th International Conference on CVD,* 87-88, 625 (1987).
19. T. Ohba, S. Inoue and M. Maeda, *Proc. IEEE IEDM Tech. Dig.* 213 (1987).
20. R. Foster, S. Tseng, L. Lane and K. Ahn, *Tungsten and Other Refractory Metals for VLSI Applications III,* edited by V. A. Wells (Materials Research Society, Pittsburgyh, 1988), p. 69.
21. H. H. Busta and C. H. Tang, *J. Electrochem. Soc.* **133**, 1195 (1986).
22. K. J. Laidler, Catalysis, Edited by P. H. Emmet (Reinhold publishing Co., 1954) Vol. 1, Chapt. 4, pp. 119-196; G. C. Bond, *Heterogeneous catalysis: principles and applications* (Clarendon Press, Oxford, 1986).
23 D. D. Wagman, W. H. Evans, V. B. Parker, R. H. Schumm, I. Halow, S. M. Bailey, K. L. Churney and R. L. Nuttal, *J. Phys.* Chem. Ref. Data 11, Suppl. 2 (1982).
24 J. D. McDonald, C. H. Williams, J. C. Thompson and J. L. Margrace, *Advan. Chem, Ser.* **72**, 261 (1968).
25 Joint Army-Navy-Air Force, *Thermochemical Tables* (1961).
26 D. L. Hildenbrand, *J. Chem. Phys.* **62**, 3974 (1975).
27 V. S. Pervov and A. V. Gusarov, *Izv. Akad. Nauk SSSR. Neorg. Mater.* **12**, 133 (1976).